

## Enhanced outcoupling from organic light-emitting diodes using aperiodic dielectric mirrors

Mukul Agrawal

*Electrical Engineering, Stanford University, California 94305*

Yiru Sun

*Electrical Engineering, Princeton University, Princeton, New Jersey 08544*

Stephen R. Forrest

*Electrical Engineering and Computer Science and Physics, University of Michigan, Ann Arbor, Michigan 48109*

Peter Peumans<sup>a)</sup>

*Electrical Engineering, Stanford University, California 94305*

(Received 23 April 2007; accepted 22 May 2007; published online 14 June 2007)

Aperiodic dielectric stacks between the substrate and transparent anode in organic light-emitting diodes are used to improve the optical outcoupling efficiency. The authors demonstrate that a nine-layer  $\text{SiO}_2/\text{SiN}_x$  aperiodic dielectric stack improves the brightness by 80% within a  $60^\circ$  viewing cone for a red-emitting organic light-emitting diode, while maintaining a Lambertian emission pattern. As the refractive index contrast between the two materials used in a two-component multilayer dielectric stack is increased, a brightness improvement of 170% in a  $60^\circ$  viewing cone is achievable while maintaining a Lambertian emission profile. © 2007 American Institute of Physics. [DOI: 10.1063/1.2748859]

Organic light-emitting diodes (OLEDs) are efficient and tunable thin-film light sources with applications in displays and solid-state lighting.<sup>1–9</sup> The luminous efficiency, lifetime, and color gamut of both small molecular weight and polymer OLEDs have continuously increased since the demonstration of efficient electroluminescence in an organic heterostructure.<sup>1</sup> Despite this progress, a large fraction of the optical energy generated in an OLED is wasted since it couples into modes that are substrate trapped (ST) by total internal reflection, waveguided (WG) modes, or surface plasmon polariton (SPP) modes at the metal cathode/organic interface.<sup>2–7</sup> The fraction of photons emitted into unbound (UB) modes is the outcoupling efficiency  $\eta_{\text{OC}}$ . In small molecular weight OLEDs with randomly oriented emitting dipoles,  $\eta_{\text{OC}} \approx 20\%$ , while for polymer OLEDs,  $\eta_{\text{OC}} \approx 30\%$  since in that case the emissive dipoles tend to align in the substrate plane during film deposition.<sup>7</sup>

Schemes to enhance  $\eta_{\text{OC}}$  fall into two categories. One modifies the structure or geometry of the device such that a greater fraction of the optical modes of the structure are unbound. Examples of such approaches are substrate surface texturing,<sup>2,3</sup> substrate microlenses,<sup>4,5</sup> and scattering layers.<sup>6</sup> A second approach is to alter the spatial profiles of the optical modes to increase the coupling strength of the emissive dipoles to the UB modes. This approach also modifies the spontaneous emission rate and internal quantum efficiency through the Purcell effect.<sup>8–11</sup> This approach was previously used to increase the efficiency of LEDs using both one-dimensional (1D) (Refs. 8 and 9) and two-dimensional<sup>10,11</sup> periodic photonic structures. The use of 1D periodic structures in OLEDs is limited because of the broad spontaneous emission spectra of organic emitters with a full width at half maximum (FWHM) of  $\sim 70$  nm.<sup>1–9</sup> This leads to strong variations in brightness and color with viewing angle.<sup>9</sup> Fur-

thermore, emission is enhanced only over a narrow range of wavelength and angle, and is suppressed elsewhere, leading to reduced total power efficiency for emitters with broad emission spectra.<sup>12</sup> Two-dimensional periodic structures have similar shortcomings and require high-resolution patterning.<sup>10,11</sup>

In an archetypical OLED,  $\sim 75\%$  of photons that couple to UB modes are emitted at angles  $>30^\circ$  from the device normal. Therefore, for most display applications, the useful  $\eta_{\text{OC}}$  (fraction of generated photons that are emitted within the viewing cone) of a small molecule OLED is only  $\sim 5\%$  (for a  $30^\circ$  viewing cone). We have developed a methodology based on needle optimization<sup>13,14</sup> to design two-component 1D aperiodic dielectric multilayer stacks that, when inserted between the substrate and transparent anode of an OLED, can enhance the useful  $\eta_{\text{OC}}$  up to 170%. This is achieved by modifying the spatial profiles of all bound and UB modes such that coupling of excitons to UB modes, corresponding to radiation within the viewing cone, is increased. At the same time, the coupling strength of the various UB modes is tuned such that the emission pattern remains close to Lambertian within the viewing cone, ensuring uniform pixel brightness. Substantial improvements in the brightness are achieved by the combined effects of (1) a redistribution of the photons that would otherwise be emitted outside the viewing cone and (2) a reduction of the coupling of emitted photons into the ST, the WG, and the SPP modes. A detailed description of the design methodology is described elsewhere.<sup>15</sup> The electrical and optical characteristics of the devices were evaluated using previously published methods.<sup>16–18</sup>

In Fig. 1(a), three stack designs are shown that enhance the emission within a  $60^\circ$  viewing cone for a red OLED based on the phosphor tris(1-phenylisoquinoline)-iridium (III) ( $\text{Ir}(\text{piq})_3$ ) with a peak emission wavelength of  $\lambda = 620$  nm and FWHM = 70 nm.<sup>19</sup> Stack design 1 is a 9-layer

<sup>a)</sup>Electronic mail: ppeumans@stanford.edu

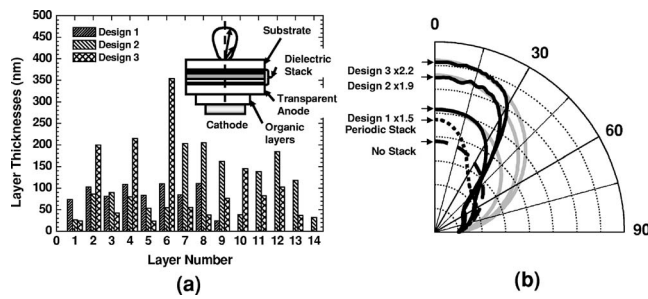


FIG. 1. (a) Aperiodic stack designs 1, 2, and 3. Stack design 1 is a 9-layer  $\text{SiO}_2/\text{SiN}_x$  stack, design 2 is a 14-layer  $\text{SnS}_2/\text{MgF}_2$  stack, and design 3 is a 13-layer  $\text{SnS}_2/\text{porous-SiO}_2$  stack. The layer closest to the transparent anode corresponds to the high index material in all three designs. Inset: Schematic of the OLED structure with aperiodic dielectric stack sandwiched between the glass substrate and transparent anode. (b) Calculated power emitted per unit solid angle as a function of azimuthal angle for designs 1, 2, and 3 (solid lines), the control OLED structure (dashed line), and an optimized periodic stack (dotted line). The scaled Lambertian response is shown for the aperiodic stack designs (gray lines).

$\text{SiO}_2/\text{SiN}_x$  stack, design 2 is a 14-layer  $\text{SnS}_2/\text{MgF}_2$  stack, and design 3 is a 13-layer  $\text{SnS}_2/\text{porous-SiO}_2$  stack. The OLED device structure [Fig. 1(a), inset] is glass substrate/dielectric stack/150 nm indium tin oxide (ITO)/30 nm  $N,N'$ -diphenyl- $N,N'$ -bis(1-naphthyl)-1-1' biphenyl-4,4' diamine (NPD)/25 nm 4,4'- $N,N'$ -dicarbazole-biphenyl (CBP):7%  $\text{Ir}(\text{piq})_3$ /40 nm 4,7-diphenyl-1,10-phenanthroline (BPhen)/0.8 nm LiF/Al.  $\text{SiN}_x$ ,  $\text{SiO}_2$ ,  $\text{SnS}_2$ , and  $\text{MgF}_2$  have  $n=1.97$ ,  $n=1.46$ ,  $n=2.6$ , and  $n=1.3$  (Refs. 20 and 21) at  $\lambda=620$  nm, respectively. It has been recently reported that porous  $\text{SiO}_2$  films<sup>22</sup> behave as a very low index material with  $n=1.08$ . The refractive index contrasts in the three designs are 1.3, 2.0, and 2.4, respectively.

Figure 1(b) shows the calculated spectrally integrated power density of emitted radiation per unit solid angle into UB optical modes at different azimuthal angles from the surface normal. We compare the performance of an OLED without a stack (dashed line) to that with an optimized periodic (dotted line) and aperiodic (solid lines) stacks of designs 1, 2, and 3. The periodic and aperiodic stacks were optimized for maximum outcoupling integrated over a  $60^\circ$  viewing cone. The design was subjected to the constraint that the angular emission profile be Lambertian within the viewing cone. While periodic stacks provide outcoupling improvements over  $\sim 10^\circ$ , outcoupling is substantially reduced at  $>10^\circ$ . This results in a reduction in the total  $\eta_{\text{OC}}$  compared to a control OLED from 20.4% to 17.7%. The optimized aperiodic stacks, on the other hand, result in a total  $\eta_{\text{OC}}=21.4\%$ , 24.6%, and 26.5% for design 1, 2, and 3, respectively. On the other hand, the brightness within the  $60^\circ$  viewing cone is enhanced by 50%, 145%, and 170% for designs 1, 2, and 3, respectively. The root mean square deviation from the ideal Lambertian distributions (gray lines) is less than 5% for all designs within the viewing cone. The aperiodic dielectric stacks do not appreciably affect the total radiative lifetime of the exciton. The total radiative decay rate (summed over UB, ST, WG, and SPP modes) changes by  $<1.7\%$  for all designs. The radiative decay rate into UB modes changes by 1.2%, 15.5%, and 25.7% for designs 1, 2, and 3, respectively, reflecting the improved coupling into the UB modes.

We fabricated a red phosphorescent OLED onto stack design 1 and on a control substrate (no dielectric stack). The

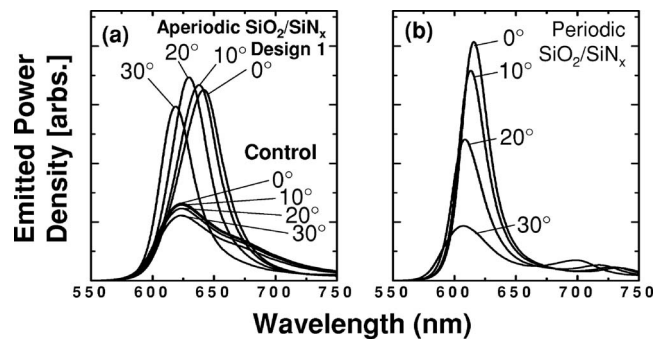


FIG. 2. (a) Calculated spectral power density at different azimuthal angles for an OLED with a nine-layer  $\text{SiO}_2/\text{SiN}_x$  stack optimized for a  $60^\circ$  viewing cone. For comparison, the response of the control OLED structure is also shown. (b) Power spectral density for an OLED with optimized periodic  $\text{SiO}_2/\text{SiN}_x$  stack.

$\text{SiO}_2/\text{SiN}_x$  dielectric stack was deposited by plasma-enhanced chemical vapor deposition on glass substrates prior to ITO deposition. The 150-nm-thick,  $20 \Omega/\text{sq}$  ITO anode was deposited by electron beam evaporation. Prior to organic layer deposition, the substrates were degreased with detergent solution and solvents, as described previously,<sup>23</sup> and were exposed to UV ozone at  $20 \text{ mW}/\text{cm}^2$  for 5 min. The organic layers were deposited in a vacuum thermal evaporation system at a base pressure  $<1 \times 10^{-7}$  Torr. The LiF/Al cathode was deposited in the same system through a shadow mask with  $1 \text{ mm}^2$  openings. Spectrally resolved optical constants for all thin films were measured on glass and Si using a spectroscopic ellipsometer. The refractive indices of the layers for  $\lambda=620$  nm are glass (1.522),  $\text{SiN}_x$  ( $1.976+0.003i$ ),  $\text{SiO}_2$  (1.463), ITO ( $1.551+0.182i$ ), NPD ( $1.771+0.004i$ ), CBP (1.806), BPhen ( $1.693+0.001i$ ), LiF (1.346), and Al ( $1.299+7.465i$ ).

The spectral density of the electroluminescence as a function of angle was measured by coupling the emitted light into a fiber mounted on a rotating arm and connected to a spectrometer. The angular emission pattern was measured at  $10 \text{ mA}/\text{cm}^2$  and using a  $0.25 \text{ cm}^2$  silicon detector mounted on a rotating arm at a distance of 7 cm from the emitter. For current density–voltage ( $J$ - $V$ ) and luminescence–voltage characterizations, the OLEDs were placed directly on top of a large area silicon detector. The measured detector current was compensated for the spectral response of the detector.

In Fig. 2(a), the calculated spectral power emitted per unit solid angle is shown versus azimuthal angle for the OLED without stack and one with the aperiodic  $\text{SiO}_2/\text{SiN}_x$  stack (design 1). Both devices show a minimal variation in power per unit solid angle as required for a Lambertian emitter, but emission from the device with the dielectric stack is 50% more intense [see Fig. 1(b)]. As shown in Fig. 2(b), the angular distribution of the spectral power of an OLED with a periodic  $\text{SiO}_2/\text{SiN}_x$  stack is sharply peaked. The vertical scales of Figs. 2(a) and 2(b) are identical. The Commission Internationale de l'Éclairage (CIE) chromaticity coordinates for the control OLED are (0.67, 0.32).<sup>19</sup> The coordinates for the OLED with the aperiodic  $\text{SiO}_2/\text{SiN}_x$  stack show a slight dependence on azimuthal angle, varying from (0.69, 0.30) at  $0^\circ$  to (0.68, 0.32) at  $30^\circ$ .

In Fig. 3(a), the measured angularly integrated electroluminescence spectrum of a control OLED (open squares) is compared with that of an OLED with the optimized  $\text{SiO}_2/\text{SiN}_x$  dielectric stack (filled squares). The measured

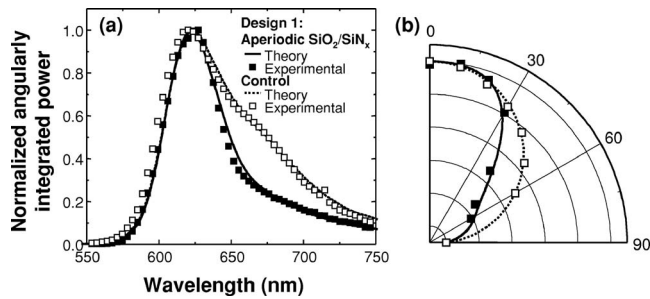


FIG. 3. Measured (symbols) and theoretically predicted (lines) angularly integrated spectral density of emitted power (a) and spectrally integrated emitted power per unit solid angle (b) for a device with nine-layer SiO<sub>2</sub>/SiN<sub>x</sub> dielectric stack (solid lines and solid symbols) and for an OLED without a dielectric stack (dotted lines and open symbols).

spectra are in agreement with theoretical predictions (solid and dotted lines). The presence of the dielectric stack results in linewidth narrowing by reduction of the long-wavelength shoulder due to suppression of dipole-field interaction. Despite this linewidth narrowing, the aperiodic microcavity structure does not reduce the spectrally and angularly integrated emitted photon flux.

The normalized (to 0° viewing angle) spectrally integrated power emitted per unit solid angle as a function of azimuthal angle from the surface normal is shown in Fig. 3(b) for an OLED with the aperiodic SiO<sub>2</sub>/SiN<sub>x</sub> stack (filled squares). For comparison, the response of the control OLED is also shown (open squares). These measurements are also in agreement with calculation (solid and dotted lines). The OLED with the dielectric stack is uniformly bright within the 60° viewing cone and lacks the sharply peaked response observed for periodic stacks.

In Fig. 4, the external quantum and power efficiencies are shown as a function of  $J$  for both the control and the nine-layer SiO<sub>2</sub>/SiN<sub>x</sub> stack device. The external quantum

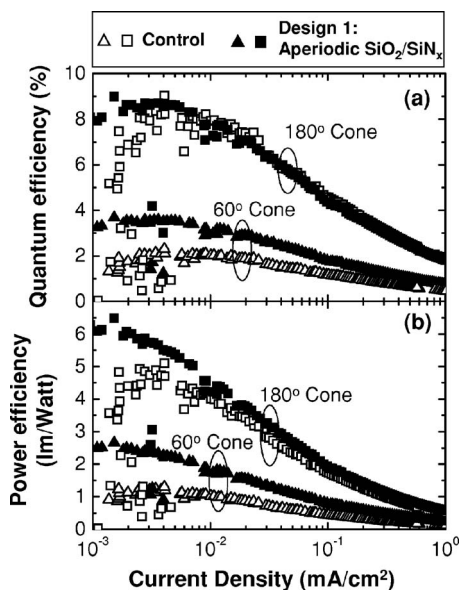


FIG. 4. Measured (a) external quantum, and (b) power efficiency vs. current density for a device with nine-layer SiO<sub>2</sub>/SiN<sub>x</sub> dielectric stack (solid symbols) and for an OLED without a dielectric stack (open symbols). Efficiencies measured within a 60° viewing cone (triangles) are compared with the efficiencies measured within the entire 180° forward half-space (squares) for both devices.

efficiency (EQE) for photons emitted in the viewing cone improves by (54±6)%, from (2.2±0.05)% to (3.4±0.05)%, in agreement with the expected enhancement of 50%, while the total EQE of (8.0±0.05)% remains unchanged. The power efficiency for photons emitted within the viewing cone increases by (81±3)% to 2.7±0.1 lm/W, while the total peak power efficiency increases by (13±5)% to 6.75±0.05 lm/W. The increase in power efficiency is larger than the enhancement in EQE due to suppression of long-wavelength shoulder in the emission spectra, providing an improved match to the eye response.

In conclusion, we have shown that aperiodic dielectric stacks can achieve significantly increased outcoupling efficiencies in OLEDs while maintaining a Lambertian emission pattern within the specified viewing cone. This is achieved by redistributing the coupling to UB modes to those modes that emit within the desired viewing cone, and by reducing coupling to the ST, WG, and SPP modes. Because the dielectric stack lies outside of the electrically active region, it can be combined with already optimized device structures without affecting electrical performance. Using a practically achievable index contrast of  $n=2.6/1.08$ , the stacks can increase the brightness of a typical OLED by a factor of 2.7 while maintaining a Lambertian emission profile within a 60° viewing cone.

The authors thank the Department of Energy Solid State Lighting Program and Universal Display Corporation for partial support of this work.

- <sup>1</sup>C. W. Tang and S. A. VanSlyke, *Appl. Phys. Lett.* **51**, 913 (1987).
- <sup>2</sup>P. A. Hobson, S. Wedge, J. A. E. Wasey, I. Sage, and W. L. Barnes, *Adv. Mater. (Weinheim, Ger.)* **14**, 1393 (2002).
- <sup>3</sup>P. T. Worthing and W. L. Barnes, *Appl. Phys. Lett.* **79**, 3035 (2001).
- <sup>4</sup>C. F. Madigan, M. H. Lu, and J. C. Sturm, *Appl. Phys. Lett.* **76**, 1650 (2000).
- <sup>5</sup>S. Moller and S. R. Forrest, *J. Appl. Phys.* **91**, 3324 (2002).
- <sup>6</sup>T. Tsutsui, M. Yashiro, H. Yokogawa, K. Kawano, and M. Yokoyama, *Adv. Mater. (Weinheim, Ger.)* **13**, 1149 (2001).
- <sup>7</sup>L. H. Smith, J. A. Wasey, and W. L. Barnes, *Appl. Phys. Lett.* **84**, 2986 (2004).
- <sup>8</sup>T. Nakayama, Y. Itoh, and A. Kakuta, *Appl. Phys. Lett.* **63**, 594 (1993).
- <sup>9</sup>T. Tsutsui, N. Takada, and Shogo Saito, *Appl. Phys. Lett.* **65**, 1868 (1994).
- <sup>10</sup>S. Fan, P. R. Villeneuve, and J. D. Joannopoulos, *Phys. Rev. Lett.* **78**, 3294 (1997).
- <sup>11</sup>J. Vuckovic, M. Loncar, and A. Scherer, *IEEE J. Quantum Electron.* **36**, 1131 (2000).
- <sup>12</sup>A. Dodabalapur, L. J. Rothberg, R. H. Jordan, T. M. Miller, R. E. Slusher, and Julia M. Phillipse, *J. Appl. Phys.* **80**, 6954 (1996).
- <sup>13</sup>B. T. Sullivan and J. A. Dobrowolski, *Appl. Opt.* **35**, 5484 (1996).
- <sup>14</sup>A. V. Tikhonravov, M. K. Trubetskov, and G. W. DeBell, *Appl. Opt.* **35**, 5493 (1996).
- <sup>15</sup>M. Agrawal and P. Peumans *Opt. Express* (to be published).
- <sup>16</sup>G. W. Ford and W. H. Weber, *Phys. Rep.* **113**, 195 (1984).
- <sup>17</sup>R. R. Chance, A. Prock, and R. Silbey, *Adv. Chem. Phys.* **37**, 16 (1978).
- <sup>18</sup>V. Bulovic, V. B. Khalfin, G. Gu, and P. E. Burrows, *Phys. Rev. B* **58**, 3730 (1998).
- <sup>19</sup>A. Tsuboyama, H. Iwawaki, M. Furugori, T. Mukaide, J. Kamatani, S. Igawa, T. Moriyama, S. Miura, T. Takiguchi, S. Okada, M. Hoshino, and Kazunori Ueno, *J. Am. Chem. Soc.* **125**, 12971 (2003).
- <sup>20</sup>*Handbook of Optical Constants of Solids*, edited by E. D. Palik, (Academic, Boston, 1999), 1, 7819–774.
- <sup>21</sup>M. Deopura, C. K. Ullal, B. Temelkuran, and Y. Fink, *Opt. Lett.* **26**, 1197 (2001).
- <sup>22</sup>J. S. Juneja, *Opt. Lett.* **31**, 601 (2006).
- <sup>23</sup>R. J. Holmes, B. W. D'Andrade, X. Ren, M. E. Thompson, and S. R. Forrest, *Appl. Phys. Lett.* **83**, 3818 (2003).